The Use of Intensity-Based Measures to Produce Image Function Metrics Which Accommodate Weber's Models of Perception

Dongchang Li[1], Davide La Torre[2,3], and Edward R. Vrscay[1(✉)]

[1] Department of Applied Mathematics, Faculty of Mathematics, University of Waterloo, Waterloo, ON N2L 3G1, Canada
d235li@edu.uwaterloo.ca, ervrscay@uwaterloo.ca
[2] Dubai Business School, University of Dubai, 14143 Dubai, UAE
dlatorre@ud.ac.ae
[3] Department of Economics, Management and Quantitative Methods, University of Milan, 20122 Milan, Italy
davide.latorre@unimi.it

Abstract. We are concerned with the construction of "Weberized" metrics for image functions – distance functions which allow greater deviations at higher intensity values and lower deviations at lower intensity values in accordance with Weber's models of perception. In this paper, we show how the use of appropriate nonuniform measures over the image function range space can be used to produce "Weberized" metrics. In the case of Weber's standard model, the resulting metric is an L^1 distance between logarithms of the image functions. For generalized Weber's law, the metrics are L^1 distances between appropriate powers of the image functions. We then define the corresponding L^2 analogues of these metrics which are easier to work with because of their differentiability properties. Finally, we extend the definition of these "Weberized" metrics to vector-valued functions.

1 Introduction

It is well known that the commonly used mean squared error (MSE) and PSNR – both examples of L^2-based measures – perform poorly in terms of perceptual image quality [4,12]. This paper represents a continuation of earlier research [5] on methods of modifying L^2-based approximations so that they conform better to Weber's model of perception. A number of papers have incorporated Weber's model into classical image processing methods, thereby "Weberizing" them, e.g., total variation (TV) restoration [9] and Mumford-Shah segmentation [10].

One way to "Weberize" the L^2 distance between two functions u and v – or any metric involving an integration over some power of the differences $|u(x) - v(x)|$ – is to employ an *intensity-based weight function* in which regions of higher (lower) intensity values have a lower (higher) weight. A simple, seemingly *ad hoc*, yet effective method introduced in [5] is to divide the difference $|u(x) - v(x)|$ by

A. Campilho et al. (Eds.): ICIAR 2018, LNCS 10882, pp. 326–335, 2018.
https://doi.org/10.1007/978-3-319-93000-8_37

$|u(x)|$ or $|v(x)|$. If we use $|u(x)|$ and consider $v(x)$ to be an approximation to $u(x)$, we obtain the following "Weberized L^2" distance function,

$$\Delta(u,v) = \int_X \left[1 - \frac{v(x)}{u(x)}\right]^2 dx, \tag{1}$$

where X is the support of the image functions. This distance function is convenient to employ: If $v(x)$ is a linear combination of basis functions, the minimization of $\Delta(u,v)$ yields a linear system in the expansion coefficients c_k [5].

Minimization of $\Delta(u,v)$ in Eq. (1) is also consistent with the notion that Weber's model is better accommodated when one considers *ratios* of signal/image functions u and v as we discuss in more detail below.

In this paper, we examine another method of producing Weberized distance functions, namely by employing appropriate nonuniform *measures* over the greyscale intensity space. This idea, introduced in [3], was employed in [5] to show that the logarithmic L^1 distance between two functions u and v conforms to Weber's model. In contrast to [5], however, we consider a generalized family of Weber's models of perception: Given a greyscale background intensity $I > 0$, the minimum change in intensity ΔI perceived by the human visual system (HVS) is related to I as follows,

$$\frac{\Delta I}{I^a} = C, \tag{2}$$

where $a > 0$ and C is constant, or at least roughly constant over a significant range of intensities I [11]. In practically all applications, $a = 1$, the standard Weber model. There are, however, situations, in which other values of a, in particular, $a = 0.5$, may apply – see, for example, [7]. Equation (2) suggests that the HVS will be less/more sensitive to a given change in intensity ΔI in regions of an image at which the local image intensity $I(x)$ is high/low. As such, a Weberized distance between two functions u and v should tolerate greater/lesser differences over regions in which they assume higher/lower intensity values. The degree of toleration will be determined by the exponent a in Eq. (2).

Indeed, such a "Weberization" is built into well-known structural similarity (SSIM) measure [12,13], which demonstrates superior performance in comparison with MSE and PSNR as well as other image quality measures in terms of perceptual quality. Its luminance term, denoted as $S_1(\mathbf{x},\mathbf{y})$, characterizes the similarity between the mean values, $\bar{\mathbf{x}}$ and $\bar{\mathbf{y}}$ of two image patches $\mathbf{x}$ and $\mathbf{y}$, respectively. S_1 is a rational function $\bar{\mathbf{x}}$ and $\bar{\mathbf{y}}$ which can be rewritten as a function of the ratio $\bar{\mathbf{y}}/\bar{\mathbf{x}}$ (or $\bar{\mathbf{x}}/\bar{\mathbf{y}}$). If $\mathbf{y}$ is an approximation to $\mathbf{x}$ then greater deviations between $\bar{\mathbf{y}}$ and $\bar{\mathbf{x}}$ will be tolerated when $\bar{\mathbf{x}}$ is greater.

The primary purpose of this paper is to provide the mathematical basis for the construction of various "Weberized" image function metrics using intensity-based measures. This, in turn, is a particular case of the more general mathematical problem of what may be call "range-based function approximation." To the best of our knowledge, this is the first time that range-based measures have been employed in function approximation. We acknowledge that the rather elaborate strategy described in this paper could, in practice, be bypassed by means

of standard "patch-based" methods. Indeed, earlier work on a best SSIM-based approximation method [2] may be viewed as a "patch-based" intensity-dependent approximation method. That being said, the history of signal and image processing clearly shows the numerous benefits of pursuing more general mathematical formalisms, in terms of both theory as well as applications, and we hope that this paper will inspire future efforts in both.

We summarize the basic mathematical ingredients of our formalism:

1. The **base (or pixel) space** $X \subset \mathbb{R}$ on which our signals/images are supported. In practical computations, we shall assume, unless otherwise indicated, that $X = [0, 1]$ or $[0, 1]^2$. In the case of digital images, X can be the set of pixel locations (i, j), $1 \leq i \leq n_1$, $1 \leq j \leq n_2$.
2. The **greyscale range** $\mathbb{R}_g = [A, B] \subset (0, \infty)$.
3. The **signal/image function space** $\mathcal{F} = \{u : X \to \mathbb{R}_g \mid u \text{ is measurable}\}$. Note that from our definition of the greyscale range $\mathbb{R}_g$, $u \in \mathcal{F}$ is positive and bounded, i.e., $0 < A \leq u(x) \leq B < \infty$ for all $x \in X$. A consequence of this boundedness is that $\mathcal{F} \subset L^p(X)$ for all $p \geq 1$, where the $L^p(X)$ function spaces are defined in the usual way. For any $p \geq 1$, the L^p norm can be used to define a metric d_p on $\mathcal{F}$: For $u, v \in \mathcal{F}$, $d_p(u, v) = \|u - v\|_p$. Our primary concern is the approximation of functions in the case $p = 2$, i.e., the Hilbert space, $L^2(X)$, with metric,

$$d_2(u, v) = \|u - v\|_2 = \left[\int_X [u(x) - v(x)]^2 \, dx\right]^{1/2}, \quad u, v \in L^2(X). \tag{3}$$

2 Distance Functions Generated by Measures on the Greyscale Range Space $\mathbb{R}_g$

With reference to the notation introduced in the previous section, we now describe a method of generating intensity-dependent metrics between functions in the space $\mathcal{F}$ by using measures that are supported on the bounded range space $\mathbb{R}_g = [A, B]$. In what follows, we let the base space be $X = [a, b]$.

Consider two functions $u, v \in \mathcal{F}$ and define the following subsets of X,

$$X_u = \{x \in X \mid u(x) \leq v(x)\} \qquad X_v = \{x \in X \mid v(x) \leq u(x)\}, \tag{4}$$

so that $X = X_u \cup X_v$. A possible situation is sketched in Fig. 1 below.

The goal is to assign a distance D between u and v based on an integration over vertical strips of width dx and centered at $x \in [a, b]$. Two such strips, one lying in the set X_u and the other in X_v, are shown in Fig. 1. In most, if not all, traditional integration-based metrics, e.g., the L^p metrics for $p \geq 1$, the contribution of each strip to the integral will be an appropriate power of the height of the strip, $|u(x) - v(x)|$. This implicitly assumes a *uniform* weighting along the intensity axis since the term $|u(x) - v(x)|$ represents the Lebesgue measure of the intervals $(u(x), v(x)]$ or $(v(x), u(x)]$.

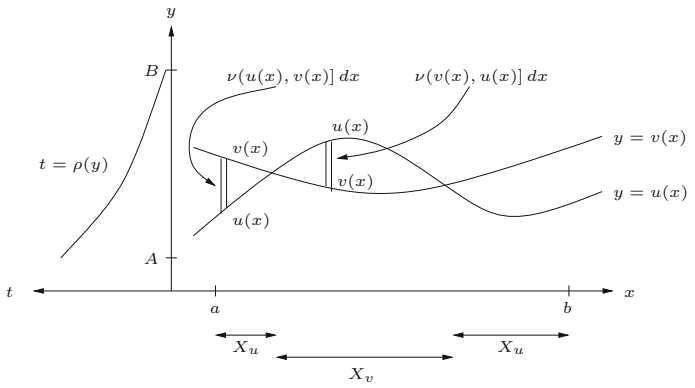

Fig. 1. Sketch of two nonnegative greyscale functions $u(x)$ and $v(x)$ with strips of width dx that will contribute to the distance $D(u, v; \nu)$.

In this study, however, the contribution of each strip will **not**, in general, be determined by the heights of the strips, i.e., the quantities $|u(x) - v(x)|$, but rather the **sizes** of the intervals $(u(x), v(x)] \subset \mathbb{R}_g$ and $(v(x), u(x)] \subset \mathbb{R}_g$ as assigned by a **measure** ν that is supported on the greyscale interval $\mathbb{R}_g = [A, B]$. The measures of the two intervals shown in the figure will be denoted as $\nu(u(x), v(x)]$ and $\nu(v(x), u(x)]$, respectively. (Note that we consider half-open intervals of the form $(y_1, y_2]$. We omit a discussion of the technical points underlying this choice.) The distance between u and v associated with the measure ν is now defined as follows,

$$D(u, v; \nu) = \int_{X_u} \nu(u(x), v(x)]\,dx \; + \; \int_{X_v} \nu(v(x), u(x)]\,dx, \tag{5}$$

Special Case: In the case that ν is the usual (uniform) Lebesgue measure on $\mathbb{R}_g$, to be denoted as m_g, the sizes of the intervals shown in Fig. 1 become $m_g(u(x), v(x)] = v(x) - u(x)$ and $m_g(v(x), u(x)] = u(x) - v(x)$, so that

$$\begin{aligned} D(u, v, m_g) &= \int_{X_u} [v(x) - u(x)]\,dx + \int_{X_v} [u(x) - v(x)]\,dx \\ &= \int_X |u(x) - v(x)|\,dx, \end{aligned} \tag{6}$$

the L^1 distance between u and v.

The natural question is, "What other kind of greyscale measures ν can/should be considered on the greyscale range $\mathbb{R}_g$?" Firstly, it is convenient to consider measures which are defined by continuous, non-negative density functions $\rho(y)$. (Such measures will be *absolutely continuous* with respect to Lebesgue measure.) Given a measure ν with density function ρ, then for any interval $(y_1, y_2] \subset \mathbb{R}_g$,

$$\nu\,(y_1, y_2] = \int_{y_1}^{y_2} \rho(y)\,dy \; = P(y_2) - P(y_1), \tag{7}$$

where $P'(y) = \rho(y)$. The distance function $D(u, v; \nu)$ in Eq. (5) then becomes

$$D(u, v; \nu) = \int_X |P(u(x)) - P(v(x))|\, dx. \tag{8}$$

Without loss of generality, we shall also assume that $\rho(y)$ is continuous on $\mathbb{R}_g$. The graph of a generic density function $\rho(y)$ supported on the interval $[A, B] \subset \mathbb{R}_g$ (y-axis) is sketched at the left of Fig. 1.

Note that the special case $\rho(y) = 1$ corresponds to Lebesgue measure on $\mathbb{R}_g$, i.e., $\nu(y_1, y_2] = y_2 - y_1$. In this case, the distance $D(u, v, \nu)$ in Eq. (8) is the L^1 distance between u and v in Eq. (6). The constancy of the density function implies that all greyscale intensity values are weighted equally. However, Weber's model of perception in Eq. (2) suggests that the density function $\rho(y)$ should be a *decreasing* function of intensity y: As the intensity value increases, the HVS will tolerate greater differences between $u(x)$ and $v(x)$ before being perceived. In [5], we presented, with a short proof, the following important result for Weber's standard model, $a = 1$:

Theorem 1: The unique measure ν on $\mathbb{R}_g$ which accommodates Weber's standard model of perception, $a = 1$ in Eq. (2), over the greyscale space $\mathbb{R}_g \subset [0, \infty)$ is, up to a normalization constant, defined by the continuous density function $\rho(y) = 1/y$. For any two greyscale intensities $I_1, I_2 \in \mathbb{R}_g$,

$$\int_{I_1}^{I_1+\Delta I_1} \frac{1}{y}\, dy = \int_{I_2}^{I_2+\Delta I_2} \frac{1}{y}\, dy \implies \nu(I_1, I_1 + \Delta I_1) = \nu(I_2, I_2 + \Delta I_2)\,, \tag{9}$$

where $\Delta I_1 = CI_1$ and $\Delta I_2 = CI_2$, are the minimum changes in perceived intensity at I_1 and I_2, respectively, according to Weber's model, $a = 1$, in Eq. (2).

Equation (9) may be viewed as an invariance result with respect to perception. Its graphical interpretation in terms of equal areas enclosed by the density curve $\rho(y)$ is shown in Fig. 2 below. The measure ν defined by the density function $\rho(y) = 1/y$ is the logarithmic measure so that the distance between u and

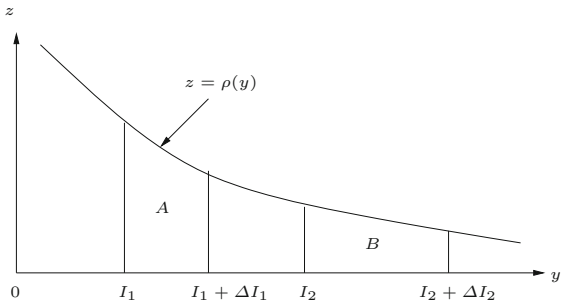

Fig. 2. Graphical interpretation of invariance result in Eq. (9). Area of A = Area of B = $\ln(1 + C)$.

v in Eq. (8) becomes

$$D(u,v;\nu) = \int_X |\ln u(x) - \ln v(x)|\, dx = \|\ln u - \ln v\|_1. \tag{10}$$

Theoretically, this is the best distance function to employ in any approximation scheme which is designed to accommodate Weber's (standard) model of perception. Unfortunately, it is difficult to work with this distance function, which leads to the consideration of more practical L^2-based analogues, as discussed in [5]. We shall discuss this further in Sect. 3 below.

We now wish to consider the generalized Weber models of perception in Eq. (2), i.e., $a \neq 1$. Once again, we expect that the density functions $\rho_a(y)$ associated with these models will be decreasing functions of y. Given that $\rho_1(y) = 1/y$, one might conjecture that the density function $\rho_a(y)$ for any $a > 0$ will be given by $\rho_a(y) = 1/y^a$. This is *asymptotically true*, as we state below.

Theorem 2: For $a > 0$, the density function $\rho_a(y)$ which accommodates Weber's model of perception in Eq. (2) is, to leading order, $\rho_a(y) \simeq 1/y^a$ as $y \to 0^+$: For any two greyscale intensities $I_1, I_2 \in \mathbb{R}_g$,

$$\int_{I_1}^{I_1+\Delta I_1} \rho_a(y)\, dy \simeq \int_{I_2}^{I_2+\Delta I_2} \rho_a(y)\, dy, \tag{11}$$

where $\Delta I_1 = CI_1^a$ and $\Delta I_2 = CI_2^a$ are the minimum changes in perceived intensity at I_1 and I_2, respectively, according to Weber's model in Eq. (2).

This result, which is a generalized version of the invariance result in Eq. (9), is derived in the Appendix. It may also be interpreted geometrically as shown in Fig. 2 with ΔI_1 and ΔI_2 defined in the statement of Theorem 2.

Theorem 2 may also be extended to include the case $a = 0$, essentially an absence of Weber's model. In this case $\rho_0(y) = 1$, so that $\nu = m_g$, Lebesgue measure on $\mathbb{R}_g$. Furthermore, the relation in (11) becomes an equality.

For $a \geq 0$, $a \neq 1$, substitution of (the leading-order approximations to) the density functions $\rho_a(y) = 1/y^a$ into Eq. (8) yields, up to a multiplicative constant, the following distance functions,

$$D_a(u,v) = D(u,v;\nu_a) = \int_X \left|u(x)^{-a+1} - v(x)^{-a+1}\right|\, dx. \tag{12}$$

Note that the special case $a = 0$ has already been presented in Eq. (6). And finally, the case $a = 1$ – Weber's standard model – was presented in Eq. (10).

In closing this section, we mention that as a increases, the density functions $\rho_a(y) = 1/y^a$ decrease more rapidly with respect to y. As such, regions of higher intensity values will contribute less to the distance functions $D(u,v;\nu_a)$. This effect will be demonstrated in a particular example in the next section.

3 Function Approximation Using Generalized Greyscale Measures ν_a

We now consider $u(x)$ to be a reference function and $v(x)$ to be an approximation to $u(x)$ having the standard form, $v(x) = \sum_{k=1}^{N} c_k \phi_k(x)$, where the set $\{\phi_k\}_{k=1}^{N}$ is assumed to be linearly independent, and perhaps orthogonal, over $X = [a, b]$. We shall denote $Y_N = \text{span}\{\phi_1, \cdots, \phi_N\}$.

Theoretically, given a $u(x) \in \mathcal{F}$ and an $a > 0$, the best Y_N-approximation of $u(x)$ in the metric space $(\mathcal{F}, D_a)$ is obtained by minimizing the distance $D(u, v; \nu_a)$ in Eq. (12). Unfortunately, these distance functions are difficult to work with, especially from a theoretical perspective, primarily because of the appearance of the absolute value in the integrand. One way to reduce such complications is to consider their L^2 analogues, defined as follows,

$$D_{2,a}(u, v; \nu_a) = \left[\int_X \left[u(x)^{-a+1} - v(x)^{-a+1} \right]^2 dx \right]^{1/2}, \quad a \neq 1, \tag{13}$$

and, for the case $a = 1$,

$$D_{2,1}(u, v; \nu_1) = \left[\int_X \left[\ln u(x) - \ln v(x) \right]^2 dx \right]^{1/2}. \tag{14}$$

We may now impose stationarity conditions on these integrals:

Case 1: $a \neq 1$. For $1 \leq p \leq N$, using Eq. (13),

$$\frac{\partial D_{2,a}}{\partial c_p} = 0 \quad \Longrightarrow \quad \int_X \left[u(x)^{-a+1} - v(x)^{-a+1} \right] \frac{\phi_p(x)}{v(x)^a} dx = 0. \tag{15}$$

Case 2: $a = 1$. For $1 \leq p \leq N$, using Eq. (14),

$$\frac{\partial D_{2,1}}{\partial c_p} = 0 \quad \Longrightarrow \quad \int_X \left[\ln u(x) - \ln v(x) \right] \frac{\phi_p(x)}{v(x)} dx = 0. \tag{16}$$

For a given $a > 0$, the equations for $1 \leq p \leq N$ in either (15) or (16) comprise an extremely complicated nonlinear system of equations in the unknown coefficients $c_1, c_2, \cdots, c_N$. Alternatively, one may employ some kind of gradient descent scheme to find the coefficients c_k which minimize the squared distance D_2. A convenient starting point for such schemes are the coefficients of the best L^2 approximation ($a = 0$) which are easily computed. Such an approach was employed in the following illustrative example.

Example 1: We consider the step function $u(x)$ with values 1 and 3 on half intervals of $X = [0, 1]$, as shown in Fig. 3. Also shown are plots of the best approximations for the cases $a = 0$ (best L^2), $a = 0.5$ and $a = 1$ (standard Weber) using the following orthonormal basis: $\phi_1(x) = 1$, $\phi_k(x) = \sqrt{2}\cos(k\pi x)$,

$2 \le k \le 5$. As expected, the approximations for $a = 0.5$ and $a = 1$ show less deviation from $u(x)$ than the best L^2 approximation over the lower intensity region $0 \le x \le 1/2$ and higher deviation over the higher intensity region $1/2 < x \le 1$. Also as expected, the deviation from $u(x)$ in the lower (higher) intensity regions decreases (increases) with increasing a since the associated density functions $\rho_a(t) = 1/t^a$ decrease more rapidly with increasing a.

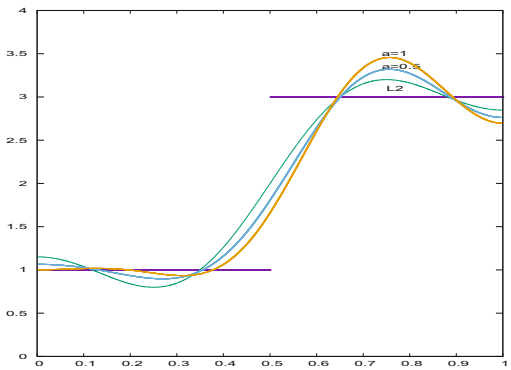

Fig. 3. Best approximations to step function $u(x)$ using $N = 5$ orthogonal cosine basis functions on [0, 1] for $a = 0$ (best L^2, green), $a = 0.5$ (blue) and $a = 1$ (standard Weber, yellow). (Color figure online)

Example 2: We consider a 256×256-pixel 8 bpp image composed of four squares with greyscale values $60, 128, 128$ and 220. In Fig. 4 are shown the best approximations for $a = 0$ (best L^2) and $a = 1$ (standard Weber) obtained with the 2D basis set $\Phi_{kl}(n, m) = \phi_k(n)\phi_k(m)$, $0 \le i, j \le 14$, where the $\phi_i(n)$ are standard DCT basis functions. The $a = 1$ approximation exhibits greater/lesser deviation at higher/lower greyscale levels than the best L^2 approximation.

4 Weber's Model for Vector-Valued Image Functions

We now consider vector-valued image functions $\mathbf{u} : X \to \mathbb{R}^N$ having the form $\mathbf{u}(x) = (u_1(x), u_2(x), \cdots, u_N(x))$, e.g., $N = 3$ for RGB color images, $N = 224$ for AVIRIS hyperspectral images [1]. We also assume that Weber's (standard) law holds for each wavelength/channel, i.e.,

$$\Delta I_k = C_k I_k\,, \quad 1 \le k \le N. \tag{17}$$

The appropriate density function for each channel is $\rho_k(y) = 1/y$ which yields the following distance between components of $u(x)$ and $v(x)$,

$$D(u_k, v_k, \nu_k) = \int_X |\ln u_k(x) - \ln v_k(x)|\, dx. \tag{18}$$

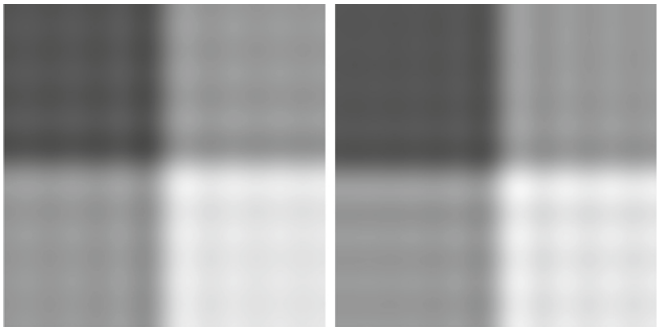

Fig. 4. Left and right, respectively: Best L^2 ($a = 0$) and best Weber ($a = 1$) approximations to step image in Example 2 of text.

This, in turn, yields the following distance function between u and v,

$$D(u, v, \nu) = \sum_{k=1}^{N} D(u_k, v_k, \nu_k) = \sum_{k=1}^{N} \int_X |\ln u_k(x) - \ln v_k(x)|\, dx$$
$$= \|\ln \mathbf{u} - \ln \mathbf{v}\|_1. \tag{19}$$

Once again, the L^2 analogue of this distance function is somewhat easier to work with,

$$D_{2,1}(u, v, \nu) = \left[\sum_{k=1}^{N} \int_X [\ln u_k(x) - \ln v_k(x)]^2\, dx\right]^{1/2}$$
$$= \|\ln \mathbf{u} - \ln \mathbf{v}\|_2. \tag{20}$$

Note: In the above treatment, the total distance function D in Eq. (19) could also be defined by a *weighted* sum of individual channel distances, $D(u_k, v_k, \nu_k)$. As well, associated each channel could be a measure ν_{a_k} with its own Weber exponent a_k and hence density function $\rho(y) = 1/y^{a_k}$.

Acknowledgments. We gratefully acknowledge that this research has been supported in part by the Natural Sciences and Engineering Research Council of Canada (ERV) in the form of a Discovery Grant. DLT and ERV dedicate this paper in memory of Prof. Bruno Forte (1928–2002), mentor, colleague and friend.

Appendix: Sketch of Proof of Theorem 2

We shall consider the "reverse" problem: Given the density function $\rho(y) = 1/y^a$, find the leading-order behaviour of $f(x)$ such that

$$F(x) = \int_x^{x+Cf(x)} \frac{1}{y^a}\, dy = K, \quad \text{constant}. \tag{21}$$

Differentiation with respect to x and a little manipulation yields the following differential equation (DE) for $f(x)$,

$$1 + Cf'(x) = \left[1 + \frac{Cf(x)}{x}\right]^a. \tag{22}$$

In the case $a = 1$, we easily find that $f(x) = x = x^1$. In the case $a = 0$, $f'(x) = 0$ which implies that $f(x) = x^0$. For $0 < a < 1$, we shall assume that for x sufficiently large, the RHS of Eq. (22) may be approximated using the binomial theorem, which yields the following DE for $f(x)$,

$$f'(x) = a\,\frac{f(x)}{x}. \tag{23}$$

The solution of this DE is, up to a constant, $f(x) = x^a$.

References

1. AVIRIS: Airborne Visible Infrared Imaging Spectrometer, Jet Propulsion Laboratory, California Institute of Technology. http://aviris.jpl.nasa.gov
2. Brunet, D., Vrscay, E.R., Wang, Z.: Structural similarity-based approximation of signals and images using orthogonal bases. In: Campilho, A., Kamel, M. (eds.) ICIAR 2010. LNCS, vol. 6111, pp. 11–22. Springer, Heidelberg (2010). https://doi.org/10.1007/978-3-642-13772-3_2
3. Forte, B., Vrscay, E.R.: Solving the inverse problem for function and image approximation using iterated function systems. Dyn. Contin. Discrete Impuls. Syst. **1**, 177–231 (1995)
4. Girod, B.: What's wrong with mean squared error? In: Watson, A.B. (ed.) Digital Images and Human Vision. MIT Press, Cambridge (1993)
5. Kowalik-Urbaniak, I.A., La Torre, D., Vrscay, E.R., Wang, Z.: Some "Weberized" L^2-based methods of signal/image approximation. In: Campilho, A., Kamel, M. (eds.) ICIAR 2014. LNCS, vol. 8814, pp. 20–29. Springer, Cham (2014). https://doi.org/10.1007/978-3-319-11758-4_3
6. Lee, S., Pattichis, M.S., Bovik, A.C.: Foveated video quality assessment. IEEE Trans. Multimed. **4**(1), 129–132 (2002)
7. Michon, J.A.: Note on the generalized form of Weber's Law. Percept. Psychophys. **1**, 329–330 (1966)
8. Oppenheim, A.V., Schafer, R.W., Stockham Jr., T.G.: Nonlinear filtering of multiplied and convolved signals. Proc. IEEE **56**(8), 1264–1291 (1968)
9. Shen, J.: On the foundations of vision modeling I. Weber's law and Weberized TV restoration. Physica D **175**, 241–251 (2003)
10. Shen, J., Jung, Y.-M.: Weberized Mumford-Shah model with Bose-Einstein photon noise. Appl. Math. Optim. **53**, 331–358 (2006)
11. Wandell, B.A.: Foundations of Vision. Sinauer, Sunderland (1995)
12. Wang, Z., Bovik, A.C.: Mean squared error: love it or leave it? A new look at signal fidelity measures. IEEE Signal Process. Mag. **26**, 98–117 (2009)
13. Wang, Z., Bovik, A.C., SHeikh, H.R., Simoncelli, E.P.: Image quality assessment: from error visibility to structural similarity. IEEE Trans. Image Process. **13**(4), 600–612 (2004)
14. Wang, Z., Li, Q.: Information content weighting for perceptual image quality assessment. IEEE Trans. Image Process. **20**(5), 1185–1198 (2011)